Theory and modeling of accelerating flames in tubes

Vitaly Bychkov,[1] Arkady Petchenko,[1] V'yacheslav Akkerman,[1,2] and Lars-Erik Eriksson[3]
[1]*Institute of Physics, Umeå University, SE-901 87, Umeå, Sweden*
[2]*Nuclear Safety Institute (IBRAE) of Russian Academy of Sciences, B. Tulskaya 52, 113191 Moscow, Russia*
[3]*Department of Thermo- and Fluid Dynamics, Chalmers University of Technology, 412 96 Göteborg, Sweden*
(Received 12 April 2005; published 11 October 2005)

The analytical theory of premixed laminar flames accelerating in tubes is developed, which is an important part of the fundamental problem of flame transition to detonation. According to the theory, flames with realistically large density drop at the front accelerate exponentially from a closed end of a tube with nonslip at the walls. The acceleration is unlimited in time; it may go on until flame triggers detonation. The analytical formulas for the acceleration rate, for the flame shape and the velocity profile in the flow pushed by the flame are obtained. The theory is validated by extensive numerical simulations. The numerical simulations are performed for the complete set of hydrodynamic combustion equations including thermal conduction, viscosity, diffusion, and chemical kinetics. The theoretical predictions are in a good agreement with the numerical results. It is also shown how the developed theory can be used to understand acceleration of turbulent flames.

DOI: 10.1103/PhysRevE.72.046307 PACS number(s): 47.20.−k, 47.27.−i, 82.33.Vx

I. INTRODUCTION

Two regimes of premixed burning are well-known: a slow subsonic regime of flame and a fast supersonic regime of detonation [1,2]. Chemical reaction propagates in these two regimes due to different physical mechanisms, and for the same fuel mixture the velocities of a flame and a detonation typically differ by three-four orders of magnitude. Still, quite often in the experiments a flame in a tube may spontaneously accelerate until it triggers detonation [1,3–8]. Acceleration of premixed flames and transition to detonation is one of the most important and, probably, one of the least understood problems in combustion science. Numerous experimental studies have demonstrated the following steps in the transition: a flame accelerates, pushes weak shocks, the shocks interact, get stronger, compress and heat the fresh fuel mixture, which finally explodes somewhere between the leading shock and the flame front and produces detonation. However, up to now there was very limited theoretical understanding of the flame acceleration, which is the reason and the most important part in the flame-detonation transition. The first explanation of the acceleration was suggested by Shelkin in the classical work [3], see also Ref. [4]; the explanation is related to the nonslip boundary conditions at the walls. As a flame front propagates from a closed tube end, the burning matter expands; it pushes a flow of the fresh fuel mixture; friction at the tube walls makes the flow nonuniform, which bends the flame front, increases the flame velocity and leads eventually to the flame acceleration. On the basis of that idea Shelkin has proposed a semiempirical criterion of flame acceleration, according to which any realistic flame with large density drop at the front is expected to accelerate from a closed tube end. However, since the time of Shelkin, there was a common opinion that flame acceleration is impossible without external turbulent flow. That was a fatal trouble for constructing the acceleration theory, because turbulent burning is a key problem of combustion science, which has not been solved yet despite of almost a century of intensive research, see, for example, Refs. [1,9–20]. In addition, if we forget the complications due to burning, still much controversy remains about turbulence itself even in the simplest classical configurations such as flows in tubes [21,22]. By this reason, Shelkin's explanation of the flame acceleration has not been transformed into a theory, which could describe the process and predict the acceleration parameters. Moreover, as the combustion science developed further, other candidates for the explanation of accelerating flames appeared. One of them was the hydrodynamic Darrieus-Landau (DL) instability of the flame front [1,2], which corrugates an initially planar flame front and increases the flame velocity. For a long time it was unknown, how strong the flame acceleration because of the instability may be. Recent results on the nonlinear stage of the DL instability with realistic density drop at the front have shown that in the case of limited hydrodynamic length scale (e.g., for flames in tubes) the acceleration is too weak and too short to provide the detonation triggering for realistic flame parameters [23–25]. Of course, the DL instability may lead to unlimited acceleration in the opening [25–27], but the shock waves generated by a flame in the opening diverge and decay. Another acceleration mechanism was proposed in Ref. [28], which is coupled to the transition from statistically spherical to statistically planar geometry of flame propagation on the early stages of burning in tubes just after ignition. This mechanism works also for a very short time; it fails as soon as the flame touches a tube wall. Finally, in a sequence of papers, Sivashinsky with co-authors has discussed one more mechanism of flame transition to detonation due to the hydraulic resistance, see Ref. [29], and references therein. The mechanism of hydraulic resistance studied in Ref. [29] is one dimensional, which was already quite different from the intrinsically multidimensional scenario proposed by Shelkin [3]. As a result, because of the mathematical difficulties coupled to the turbulent burning, Shelkin's explanation of accelerating flames was put aside for a long time, and it has not been developed into a theory.

Only recently a constructive idea was suggested [30,31] that turbulence plays a supplementary role in the accelera-

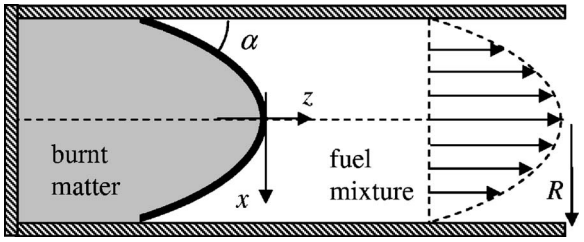

FIG. 1. A flame in a tube with nonslip at the walls.

tion, which is possible even for laminar flames with nonslip at the tube walls. The idea was probed in a few numerical simulation runs and revived the interest to the Shelkin explanation of flame acceleration. The idea of laminar flame acceleration is incredibly helpful for the theory because it allows the understanding of the effect independently of the unsolved problems of turbulent combustion. Unfortunately, the numerical studies [30,31] were too limited and provided little information beyond the fact that laminar flames can accelerate.

Here we develop the analytical theory of the flame acceleration, which explains the effect and predicts its main tendencies. According to the theory, flames with realistically large density drop at the front accelerate exponentially from a closed end of a tube with nonslip at the walls. The acceleration is unlimited until a flame triggers detonation. We find the analytical formulas for the acceleration rate, for the flame shape and for the velocity profile in the flow pushed by the flame. We validate the theory by extensive numerical simulations. The numerical simulations are performed for the complete set of combustion equations including thermal conduction, viscosity, diffusion and chemical kinetics. The theoretical predictions are in a good agreement with the numerical results. We also show how our theory can be used to understand acceleration of turbulent flames.

II. THEORY OF ACCELERATING FLAMES

To be particular, we consider a laminar flame propagating in a two-dimensional (2D) tube of half-width R with adiabatic walls and nonslip at the walls as shown schematically in Fig. 1. Burning matter expands as it passes the flame front; density ratio of the fuel mixture ρ_f and the burnt gas ρ_b is typically rather large, $\Theta=\rho_f/\rho_b=5-8$. Because of the thermal expansion, a flame propagating from the closed tube end pushes the fresh fuel mixture and generates a flow. As we have found below in the numerical simulations, the stream ahead of the flame may be well approximated by a plane-parallel flow along the walls $\mathbf{u}=\hat{\mathbf{e}}_z u_z(x,t)$. In the theory we assume the flow ahead of the flame to be exactly plane parallel. Of course, a solution obtained in such a way is only an approximate one. In order to describe dynamics of a thin flame front rigorously one has to solve the gas-dynamic equations in the fuel mixture and in the burnt matter, and to match the solutions at the flame front [25,32–34]. A solution obtained in that way takes into account a large number of different effects such as the DL instability. However, the complete rigorous solution of gas-dynamic flame equations is an extremely difficult problem, which has been solved so far only in some asymptotic limits and/or under simplifying assumptions. Making the assumption of a plane-parallel flow of the fuel mixture we may describe only the flame acceleration because of the boundary conditions, but cannot take into account the DL instability [1,4,25]. Still, the flame acceleration because of the nonslip at the walls is so strong, that the instability working in the same geometry provides only tiny corrections to the burning rate. As we will see below, our assumption works quite well in the case of well-developed flame acceleration. On the contrary, contribution of the DL instability may be significant in the very beginning of the acceleration process.

In the theory we use the traditional approach of an infinitely thin flame front propagating locally with normal velocity U_f with respect to the fuel mixture [1,4,25]. The normal velocity U_f may be treated as a hydrodynamic constant determined by thermochemical parameters of a particular fuel mixture. However, the total burning rate U_w is different from the normal velocity U_f: it shows how much fuel mixture is consumed per unit time by the whole flame front and how much energy is produced. As a result, the larger the flame surface area in comparison with the tube cross section, the larger the burning rate. In the chosen 2D geometry the relative increase in the burning rate is simply equal to the increase in the total length D_f of the flame front $U_w/U_f=D_f/2R$. Because of the flame propagation, 2D "volume" of the burning gas increases by $(\Theta-1)2RU_w$ per unit time, which generates a flow with the average velocity

$$\langle u_z\rangle=(\Theta-1)U_w, \tag{1}$$

where $\langle\cdots\rangle$ designates averaging over the tube cross section. The generated flow is not uniform. Friction stops the gas close to the walls, while flow velocities at the tube axis are larger than the average one. The nonuniform velocity profile distorts the flame shape, which leads to the flame acceleration. As we show below, asymptotically in time the flame accelerates exponentially,

$$U_w\propto\exp(\sigma U_f t/R). \tag{2}$$

The dimensionless acceleration rate σ is an eigenvalue, which has to be found from the problem solution.

To simplify the analytical calculations we introduce standard scaling choosing R, U_f, and R/U_f as units of length, velocity and time. In that case we work with the dimensionless values $(\eta;\xi)=(x;z)/R$, $\tau=tU_f/R$, $\mathbf{w}=\mathbf{u}/U_f$, $\Omega_w=U_w/U_f$, $\delta_f=D_f/R$. The scaled burning rate is coupled to the scaled length of the flame front as $\Omega_w=\delta_f/2$, the average velocity of the flame-generated flow is $\langle w_z\rangle=(\Theta-1)\Omega_w$, and the exponential acceleration of the flame front is described as $\Omega_w\propto\exp(\sigma\tau)$. A plane-parallel flow ahead of the flame front obeys the Navier-Stokes equation

$$\frac{\partial w_z}{\partial\tau}=-\frac{\partial p}{\partial\xi}+\frac{1}{\mathrm{Re}}\frac{\partial^2 w_z}{\partial\eta^2}, \tag{3}$$

where the pressure gradient is produced by the flame front, the density and pressure are scaled by ρ_f and $\rho_f U_f^2$, respectively. The value $\mathrm{Re}=RU_f/\nu$ plays the role of the

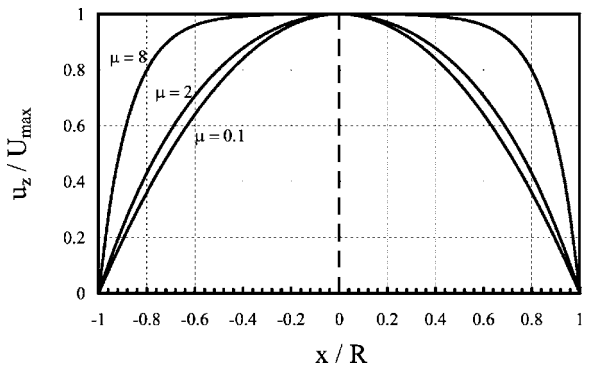

FIG. 2. The velocity profile u_z, Eq. (8), scaled by the amplitude $U_{\max}$ for different values of the parameter μ: $\mu=0.1;2;8$.

Reynolds number for the problem. In the case of a plane-parallel flow the pressure gradient is a function of time only $-\partial p/\partial\xi=\Pi(\tau)$. For usual almost isobaric burning with characteristic velocities much lower than the sound speed, the weak shocks pushed by the flame have the properties of linear acoustic waves. Then pressure perturbations are proportional to the increase in the burning rate with $\Pi(\tau)\propto\Omega_w(\tau)$. Taking into account the exponential regime of flame acceleration, the Navier-Stokes equation for $w_z(\eta,\tau)=\varphi(\eta)\exp(\sigma\tau)$ reduces to an equation for the velocity profile $\varphi(\eta)$

$$\mu^2\varphi = C_\Pi + \varphi'', \tag{4}$$

where $\mu=\sqrt{\sigma\mathrm{Re}}$. The constant C_Π comes to Eq. (4) because of forcing $\Pi(\tau)$ and it may be calculated from Eq. (1). Using the nonslip boundary conditions $\varphi=0$ at $\eta=\pm1$ we find the solution to Eq. (4)

$$\varphi = \Omega\frac{\cosh\mu-\cosh(\mu\eta)}{\cosh\mu-1}, \tag{5}$$

where we have introduced a more convenient amplitude Ω instead of the constant C_Π. Thus we obtain the velocity profile generated by the accelerating flame

$$w_z = \Omega\exp(\sigma\tau)\frac{\cosh\mu-\cosh(\mu\eta)}{\cosh\mu-1}. \tag{6}$$

Averaging Eq. (6) along the flame front and taking into account Eq. (1) we find

$$(\Theta-1)\Omega_w = \Omega\exp(\sigma\tau)\frac{\cosh\mu-\mu^{-1}\sinh\mu}{\cosh\mu-1}. \tag{7}$$

Then the velocity profile pushed by the flame becomes

$$w_z = (\Theta-1)\Omega_w\frac{\cosh\mu-\cosh(\mu\eta)}{\cosh\mu-\mu^{-1}\sinh\mu}. \tag{8}$$

Figure 2 presents the characteristic velocity profile (8) plotted for $\mu=0.1,2,8$. For relatively large value $\mu=8$ the flow resembles qualitatively a combination of two boundary layers at the walls separated by the main stream, which is practically uniform. Still, there is an important difference between a boundary layer and the flow we have obtained. Width of a boundary layer between a uniform stream and a planar wall grows along the wall [2]. On the contrary, in the flow generated by the accelerating flame, the velocity profile and the width of the transitional layers do not change with distance from the flame. In that sense the accelerating flow resembles the classical Poiseuille flow of a viscous fluid in a tube. We can reproduce the Poiseuille result from Eq. (8) taking infinitely slow acceleration of a flame front ($\sigma\to0,\mu\to0$). We can see the same parabolic dependence in Fig. 2 for $\mu=0.1$. The case of $\mu=2$ is an intermediate one between large and small values of μ, but even for $\mu=2$ the velocity profile differs only slightly form the Poiseuille solution.

The flame shape (and the burning rate) is controlled by relative motion of different parts of the flame front. Every piece of the front moves because of two reasons: (1) it propagates with respect to the fuel mixture with normal velocity; (2) it is drifted by the flow. For example, the flat top of the flame at the axis moves with the scaled velocity $1+w_z(0,\tau)$. We describe the flame shape with respect to the top point by the scaled function $f(\eta,\tau)=F/R$ defined by use of the flame position $\xi_f(\eta,\tau)$ as $\xi_f=\xi_f(0,\tau)+f(\eta,\tau)$ with $f(0,\tau)=0$ at the flame top by definition. If a small piece of the flame front is inclined, then it sweeps more fuel mixture per unit time because of the increased surface area as $[1+(\partial f/\partial\eta)^2]^{1/2}$. In addition, the front piece is drifted by the flow, which leads to local propagation velocity along the walls $w_z+[1+(\partial f/\partial\eta)^2]^{1/2}$. This velocity is different from the velocity of the flame top, and the flame shape gets distorted as

$$-\frac{\partial f}{\partial\tau} = w_z(0,\tau)-w_z+1-\left[1+\left(\frac{\partial f}{\partial\eta}\right)^2\right]^{1/2}. \tag{9}$$

Equations similar to Eq. (9) are quite typical in the nonlinear science. As an example, it has many common features with the eikonal equation, which describes interfaces growing in a turbulent flow [11] (known also as the G equation in combustion theory). However, the important difference between Eq. (9) and the eikonal equation is that the flow in Eq. (9) is determined by burning in a self-consistent way, while in Ref. [11] it may be prescribed "by hands" independent of the spreading interface. The last term in Eq. (9) is well known in the theory of turbulent flames and the DL instability as the kinematic Huygens stabilization of flame wrinkles [1,4,11,13,20,23,25,35–38]. The physical mechanism of such stabilization is that inclined parts of the front try to catch up with the flat top due to the geometric velocity increase, $[1+(\partial f/\partial\eta)^2]^{1/2}-1>0$. Obviously, we have the same tendency for accelerating flames in Eq. (9). However, in the present case the velocity shear because of the nonslip at the walls $w_z(0,\tau)-w_z$ distorts the flame so strongly that the Huygens mechanism is unable to stop the acceleration. After some transition time we have $(\partial f/\partial\eta)^2\gg1$ almost everywhere, which makes the Huygens term in Eq. (9) linear and eliminates the possibility of a nonlinear stabilization. Of course, we would like to stress that the condition of a strongly inclined front $(\partial f/\partial\eta)^2\gg1$ is not valid in the flat region around the flame top. Still, the flat region does not influence the increase of the burning rate and does not affect the analytical theory. Then Eq. (9) reduces to

$$-\frac{\partial f}{\partial \tau} = w_z(0,\tau) - w_z - \left|\frac{\partial f}{\partial \eta}\right|. \tag{10}$$

Due to the problem symmetry with respect to the axis $\eta=0$ in the following we may consider only the domain $\eta>0$, where $\partial f/\partial\eta<0$ and $|\partial f/\partial\eta| = -\partial f/\partial\eta$. Then the burning rate Ω_w becomes proportional to the flame amplitude

$$\Omega_w(\tau) = \frac{\delta_f}{2} = \int_0^1 \left[1 + \left(\frac{\partial f}{\partial \eta}\right)^2\right]^{1/2} d\eta$$

$$\approx \int_0^1 \left|\frac{\partial f}{\partial \eta}\right| d\eta = -f(1,\tau) \tag{11}$$

and Eq. (10) takes the form

$$-\frac{\partial f}{\partial \tau} = w_z(0,\tau) - w_z + \frac{\partial f}{\partial \eta}. \tag{12}$$

Since Eq. (12) is linear, then it has the solution in the form of exponential acceleration in time

$$f(\eta,\tau) = \Phi(\eta)\exp(\sigma\tau). \tag{13}$$

Substituting Eqs. (6), (7), (11), and (13) into Eq. (12) we find an equation for the flame shape

$$\Phi' = -\sigma\Phi + (\Theta-1)\Phi(1)\frac{\cosh(\mu\eta)-1}{\cosh\mu - \mu^{-1}\sinh\mu}. \tag{14}$$

Integrating Eq. (14) we obtain the flame shape as

$$\Phi(\eta) = \frac{(\Theta-1)\Phi(1)\exp(-\sigma\eta)}{\cosh\mu - \mu^{-1}\sinh\mu}\int_0^\eta [\cosh(\mu\chi)-1]\exp(\sigma\chi)d\chi \tag{15}$$

or

$$\Phi = \frac{(\Theta-1)\Phi(1)\exp(-\sigma\eta)}{\cosh\mu - \mu^{-1}\sinh\mu}\left\{\frac{\exp[(\mu+\sigma)\eta]-1}{2(\mu+\sigma)} - \frac{\exp[-(\mu-\sigma)\eta]-1}{2(\mu-\sigma)} - \frac{\exp(\sigma\eta)-1}{\sigma}\right\} \tag{16}$$

or for the whole tube $-1<\eta<1$

$$\Phi = \frac{(\Theta-1)\Phi(1)}{\cosh\mu - \mu^{-1}\sinh\mu}\left(\frac{\exp(\mu|\eta|)}{2(\mu+\sigma)} - \frac{\exp(-\mu|\eta|)}{2(\mu-\sigma)} + \frac{\mu^2}{\mu^2-\sigma^2}\frac{\exp(-\sigma|\eta|)}{\sigma} - \frac{1}{\sigma}\right). \tag{17}$$

To find the acceleration rate σ we use the condition $\Phi(\eta)=\Phi(1)$ for $\eta=1$

$$\frac{\mu\cosh\mu - \sinh\mu}{\mu(\Theta-1)} = \frac{\exp\mu}{2(\mu+\sigma)} - \frac{\exp(-\mu)}{2(\mu-\sigma)} + \frac{\mu^2}{\mu^2-\sigma^2}\frac{\exp(-\sigma)}{\sigma} - \frac{1}{\sigma}. \tag{18}$$

Particularly, in the limit of large thermal expansion, leading to $\mu\gg1$, we find from Eq. (18) with the accuracy of $\exp(-\mu)$

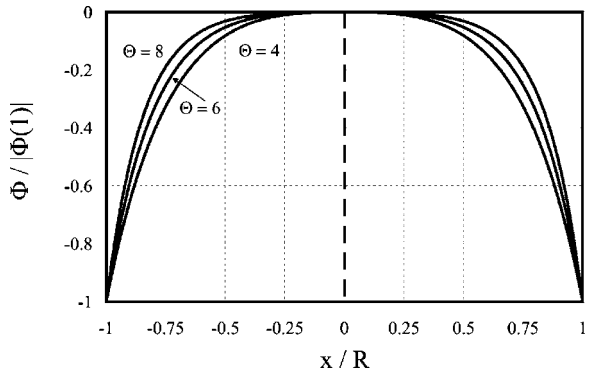

FIG. 3. The flame shape $\Phi(\eta)$, Eq. (17), scaled by $|\Phi(1)|$ for the fixed Reynolds number Re=25 and different expansion factors $\Theta=4,6,8$.

$$\mu + \sigma = (\Theta-1)\frac{\mu}{\mu-1} \tag{19}$$

or

$$\mu = \sqrt{\sigma\,\mathrm{Re}} = \frac{\mathrm{Re}-1}{2}\left(\sqrt{1+\frac{4\,\mathrm{Re}\,\Theta}{(\mathrm{Re}-1)^2}}-1\right), \tag{20}$$

with

$$\sigma = \frac{(\mathrm{Re}-1)^2}{4\,\mathrm{Re}}\left(\sqrt{1+\frac{4\,\mathrm{Re}\,\Theta}{(\mathrm{Re}-1)^2}}-1\right)^2. \tag{21}$$

In the case of large values of the Reynolds number, $\mathrm{Re}\gg4\Theta$, Eq. (21) predicts decrease of the acceleration rate σ with the Reynolds number, which becomes

$$\sigma = \Theta^2/\mathrm{Re}, \quad \mu = \Theta. \tag{22}$$

We can see that the limit of $\exp(-\mu)\ll1$ holds with a very good accuracy for flames with realistically large thermal expansion $\Theta=5-8$. Thus, in the present section we have developed the analytical theory of accelerating flames, which explains the effect, predicts the acceleration rate Eqs. (18), (21), and (22), the flame shape (17), and the velocity profile generated by the flame (8). The theoretical formula predicts a planar top of the flame front around the axis with sharp transitional regions by the walls as illustrated by Fig. 3 for the parameter values Re=25 and $\Theta=4,6,8$. Qualitatively the flame shape resembles the velocity profile, see Fig. 2.

At the end of the section it is also interesting to investigate the limits of the acceleration regime and compare them to Shelkin's criterion. In that case $\partial f/\partial\tau=0$ and Eq. (9) reduces to

$$0 = w_z(0,\tau) - w_z + 1 - \left[1+\left(\frac{\partial f}{\partial\eta}\right)^2\right]^{1/2}, \tag{23}$$

with the Poiseuille velocity profile

$$w_z = \frac{3}{2}(\Theta-1)\Omega_w(1-\eta^2) \tag{24}$$

instead of Eq. (8). The factor 3/2 comes from the relation $\max(w_z)=3\langle w_z\rangle/2$, which holds for the Pouseuille flow in the

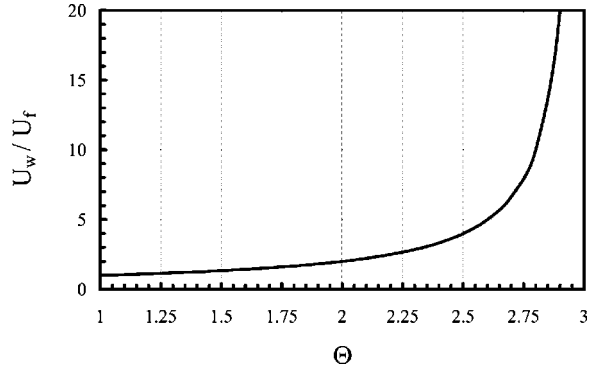

FIG. 4. The scaled velocity of a stationary flame front U_w/U_f versus the expansion factor Θ.

2D geometry. Averaging Eq. (23) over the tube cross section, we find

$$0 = w_z(0,\tau) - \langle w_z \rangle + 1 - \Omega_w. \tag{25}$$

Taking into account Eq. (1) we come to the formula for the propagation velocity of a stationary flame

$$\Omega_w = \left(1 - \frac{1}{2}(\Theta - 1)\right)^{-1}. \tag{26}$$

According to Eq. (26), stationary flame propagation is possible, if $\Theta < 3$; in the case of stronger thermal expansion flame accelerates. The propagation velocity of stationary flames is shown in Fig. 4 versus the expansion factor. As thermal expansion approaches the acceleration limit the stationary burning rate Ω_w tends to infinity. The formula (26) is similar to the Shelkin criterion of flame acceleration

$$(\Theta - 1)k_s > 1, \tag{27}$$

where the coefficient k_s shows the relative difference between the maximal and average flow velocity in a tube

$$k_s = \frac{\max(u_z)}{\langle u_z \rangle} - 1. \tag{28}$$

Shelkin evaluated the above coefficient empirically for a turbulent flow as $0.2 < k_s < 0.25$, which is comparable to our results for the laminar flow. Thus, our results are consistent with Shelkin's idea, and we have developed the idea into the rigorous theory of accelerating flames.

III. BASIC EQUATIONS OF THE DIRECT NUMERICAL SIMULATIONS

To validate the theory we have performed direct numerical simulations of the hydrodynamic combustion equations including transport processes and chemical kinetics. In the present subsection we describe the basic equations and the numerical methods used in the modeling. We use dimensional values and variables, the designations are standard for fluid mechanics. Flame dynamics obeys the following set of equations:

$$\frac{\partial \rho}{\partial t} + \frac{\partial}{\partial x_i}(\rho u_i) = 0, \tag{29}$$

$$\frac{\partial}{\partial t}(\rho u_i) + \frac{\partial}{\partial x_j}(\rho u_i u_j + \delta_{ij} p - \gamma_{ij}) = 0, \tag{30}$$

$$\frac{\partial}{\partial t}\left(\rho\varepsilon + \frac{1}{2}\rho u_i u_i\right) + \frac{\partial}{\partial x_j}\left(\rho u_j h + \frac{1}{2}\rho u_i u_i u_j + q_j - u_i \gamma_{ij}\right) = 0, \tag{31}$$

$$\frac{\partial}{\partial t}(\rho Y) + \frac{\partial}{\partial x_i}\left(\rho u_i Y - \frac{\zeta}{\mathrm{Sc}}\frac{\partial Y}{\partial x_i}\right) = -\frac{\rho Y}{\tau_R}\exp(-E/R_p T), \tag{32}$$

where Y is the mass fraction of the fuel mixture, $\varepsilon = QY + C_V T$ is the internal energy, $h = QY + C_p T$ is the enthalpy, Q is the energy release in the reaction, C_V, C_p are the heat capacities at constant volume and pressure. We consider a single irreversible reaction of first order and of the Arrhenius type with the activation energy E_a and the constant of time dimension τ_R. The stress tensor γ_{ij} and the energy diffusion vector q_j are

$$\gamma_{ij} = \zeta\left(\frac{\partial u_i}{\partial x_j} + \frac{\partial u_j}{\partial x_i} - \frac{2}{3}\frac{\partial u_k}{\partial x_k}\delta_{ij}\right), \tag{33}$$

$$q_j = -\zeta\left(\frac{C_p}{\mathrm{Pr}}\frac{\partial T}{\partial x_j} + \frac{Q}{\mathrm{Sc}}\frac{\partial Y}{\partial x_j}\right), \tag{34}$$

where $\zeta \equiv \rho\nu$ is the dynamic viscosity, Pr and Sc are the Prandtl and Schmidt numbers, respectively. The gas mixture is a perfect gas of a constant molecular weight $m = 2.9 \times 10^{-2}$ kg/mol with $C_V = 5R_p/2m$, $C_p = 7R_p/2m$, where $R_p \approx 8.31 J/(\mathrm{mol\,K})$ is the perfect gas constant. The equation of state is

$$P = \rho R_p T/m. \tag{35}$$

We consider a flame propagating in a two-dimensional tube of half-width R with adiabatic boundary conditions and with nonslip at the walls

$$\mathbf{u} = 0, \quad \hat{\mathbf{n}} \cdot \boldsymbol{\nabla} T = 0, \tag{36}$$

where $\hat{\mathbf{n}}$ is a normal vector at the wall. The flame propagates from the closed end of the tube to the open one. We take the initial pressure and temperature of the fuel mixture $P_f = 10^5$ Pa and $T = 300$ K, respectively. The thermal and chemical parameters of the fuel mixture were chosen to reproduce the most important properties of methane and propane laboratory flames. We use the dynamic viscosity $\zeta = 1.7 \times 10^{-5}$ N s/m^2, and considered two values of the Prandtl number Pr=0.5; 1. To avoid the Zeldovich (thermal-diffusion) instability we take unit Lewis number $\mathrm{Le} \equiv \mathrm{Pr}/\mathrm{Sc} = 1$. The activation energy was $E_a = 56 R_p T_f$. We took the planar flame velocity $U_f = 34.7$ cm/s and $U_f = 24.5$ cm/s for Pr=0.5 and Pr=1, respectively. These values of the planar flame velocity provided realistically slow flame propagation in comparison with the sound speed (the Mach number was about 10^{-3}). Using realistically small values for the Mach number we face extra difficulties from the numerical point of view, since large difference between the flame velocity and the sound speed increases the computa-

tional time strongly. Still, the realistically low values of the Mach number were necessary to avoid influence of gas-compression effects on the burning process and even detonation triggering, as it was in the previous papers on accelerating flames [30,31]. For comparison, in the simulations [31] the propagation velocity of the flame front close to the tube axis reached 160 m/s. The flame thickness in our calculations is defined conventionally as $L_f \equiv \nu/\mathrm{Pr}U_f$. Thermal expansion in the burning process is determined by the energy release in the reaction; we took $\Theta=8$ typical for methane and propane burning.

We use a two-dimensional Eulerian code developed in Volvo Aero. The code is robust and it was utilized quite successfully in studies of laminar burning, the hydrodynamic flame instabilities, development of corrugated flames and related phenomena, see Refs. [23,25,38]. The numerical scheme of the code and the computational methods were described in details in our previous papers [23,38]. In the present simulations we considered different tube widths $10L_f < 2R < 70L_f$, which exceeded up to 7 times the tube widths used in the previous papers on direct numerical simulations of accelerating flames [30,31]. We took the tube length much larger than the tube width $(70-110)R$, which corresponded to the tube lengths up to $2.5\times10^3 L_f$. At such large values, variations of the tube length did not influence the simulation results. We use a rectangular grid with the grid walls parallel to the coordinate axes. To perform all the calculations in a reasonable time we made the grid nonuniform along the z axis with the zone of fine grid around the flame front. In that zone the grid size was $0.2L_f$ in the z direction, which allowed us to resolve quite well the internal flame structure. Outside the region of fine grid the mesh size grows gradually with $\approx 2\%$ change in size between the neighboring cells. We employed the same method successfully in Refs. [23,38] to study the DL instability of the flame front. However, unlike the studies [23,38], in the present problem the flame is strongly curved, which results in strong increase of the burning rate. By this reason, we have much stronger numerical limitations on the tube width than in our previous studies of the DL instability. In order to keep the flame in the zone of fine grid we applied adaptive mesh moving together with the flame. Along the x axis we used a uniform grid. The number of cells in the z direction was different for different tube widths: the wider the tube, the larger the number of cells. To keep the simulation time reasonable in wide tubes we took up to 50 cells in the x direction, so that the grid size was comparable to L_f. By using such a grid we were able to resolve quite well the zone of large velocity gradients close to the walls. To check if the number of cells was sufficient for the problem, we have performed test simulation runs with number of cells increased 3 times in the x direction and obtained the same results within the accuracy of (5–10)%. This value may be considered as the numerical accuracy of our computations. Similar to our previous papers [23,38] we used the Zeldovich-Frank-Kamenetsky solution for a planar flame front as an initial condition. The planar flame front was created at a distance $12R$ from the closed tube end. Choosing other initial conditions (for example, with a strongly wrinkled flame front) we have obtained the same regime of exponential flame acceleration, but with another transition time required for the wrinkles to vanish. We kept nonreflecting boundary conditions at the open end of the tube as described in Ref. [23]. Using such conditions we avoided reflections of weak shocks and sound waves from the open end, which otherwise might influence burning and the process of flame acceleration.

One of the main dimensionless parameters of the problem is the Reynolds number defined above as $\mathrm{Re}=RU_f/\nu$. Taking into account the formula for the flame thickness L_f, we couple the Reynolds number to the scaled tube half-width R/L_f

$$\mathrm{Re} = \frac{RU_f}{\nu} = \frac{R}{\mathrm{Pr}L_f}. \tag{37}$$

By changing the tube half-width R and the Prandtl number we varied the Reynolds number within the limits $5<\mathrm{Re}<50$. Still, we would like to stress that the above definition for the Reynolds number characterizes flame dynamics. The standard definition for the Reynolds number describing the flow ahead of the flame front has another form

$$\mathrm{Re}_{\mathrm{flow}} = \frac{2R\langle u_z\rangle}{\nu} = 2(\Theta-1)\mathrm{Re}\, U_w/U_f. \tag{38}$$

The Reynolds number of the flow $\mathrm{Re}_{\mathrm{flow}}$ increases as the flame accelerates. For sufficiently large values of $\mathrm{Re}_{\mathrm{flow}}$ the stream in the tube may become turbulent. We performed the simulations as long as $\mathrm{Re}_{\mathrm{flow}}$ remained within the characteristic limits of the laminar flow. In order to study the flow turbulization properly one has to introduce the fine grid far ahead of the flame front, which would increase the computational time enormously, and which is beyond the subject of the present paper.

The main value investigated in the simulations was the scaled burning rate U_w/U_f. One can calculate the burning rate applying equation Eq. (1) sufficiently close to the flame front. To be even more accurate, in order to find U_w we have taken the difference of $\langle u_z\rangle$ ahead of the flame front and behind the front similar to Refs. [23,38]. Still, in the present problem the volume flux behind the front is about 1% and less of the flux ahead of the front and may be neglected. For every simulation run the dependence $U_w(t)$ tends (after some transition time) to the regime of exponential acceleration $U_w \propto \exp(\sigma t U_f/R)$. The exponential acceleration started typically for $U_w/U_f > 2$ or even earlier. In order to calculate the acceleration rate we eliminated the transition part of the dependence $U_w(t)$ and approximated $\ln(U_w/U_f)$ by the linear function. Since the dependencies $U_w(t)$ were not exactly exponential, the values of the acceleration rate calculated for different parts of the plot may differ. Local variations of σ did not exceed 5% for smaller values of the Reynolds number $\mathrm{Re}<25$, and they could reach as large as (10–15)% for $\mathrm{Re}>25$. This happened, first of all, because it is more difficult to achieve good computational accuracy in wider tubes corresponding to the larger values of the Reynolds number. The other reason was that the acceleration rate decreases with the Reynolds number, and the same absolute variations of σ lead to a larger relative numerical error. The variations of σ were typically smaller for $\mathrm{Pr}=0.5$ in comparison with

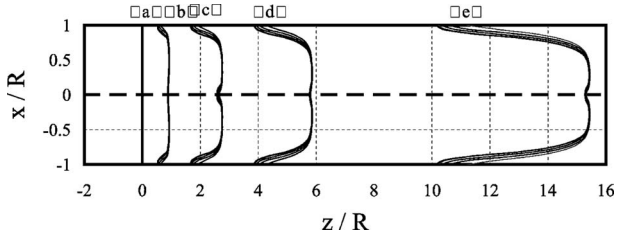

FIG. 5. Evolution of the flame isotherms (from 600 to 2100 K with the step of 300 K) in the simulation run for Re=25, the tube half-width $R=25L_f$ and the unit Prndtl number Pr=1. The positions (a), (b), (c), (d), (e) correspond to the time instants $t=(0;2.03;4,06;6.09;7.1)\times10^{-3}$ s, respectively.

Pr=1. The above uncertainty determines the accuracy of calculating the acceleration rate σ in the present paper. Remarkably, that the uncertainty in calculating σ is about the same as the estimates for the computational accuracy, which we have obtained above by changing the number of cells in the x direction.

IV. SIMULATION RESULTS

As we pointed out above, the main parameter of simulations is the Reynolds number $\mathrm{Re}=RU_f/\nu$, which we varied by changing the tube half-width R with respect to the flame thickness $L_f\equiv\nu/\mathrm{Pr}U_f$, see Eq. (37). The other parameter coming into the formula (37) for the Reynolds number is the Prandtl number. We have considered Pr=0.5; 1 in the simulations. Figure 5 shows typical evolution of the flame shape in the simulation run for Re=25, Pr=1. The flame shape is presented by isotherms 600 K$<T<$2100 K plotted with the step in temperature $\Delta T=300$ K for different time instants. As we can see, the initial planar flame becomes distorted quite fast; the flame front acquires a curved shape, which remains self-similar in the following evolution. The flame shape resembles the theoretical predictions shown in Fig. 3. To perform the quantitative comparison, we have plotted the theoretical flame shape and the isotherms obtained in the numerical simulations on one figure, Fig. 6, for Re=25, Pr=1 at the time instant $tU_f/R=1.15$. According to Fig. 6, the theoretical predictions agree quite well with the numerical results. Only two interesting features are different for the

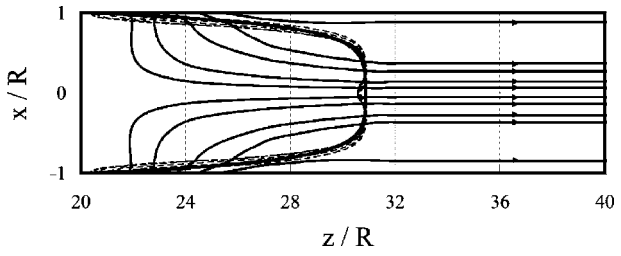

FIG. 6. Characteristic flame shape and streamlines of the flow obtained in the simulations of the present paper for Re=25, Pr=1 at the time instant $tU_f/R=1.15$. The dashed lines show the isotherms from 600 K of the fuel mixture to 2100 K of the burning products. The solid lines with arrows are the streamlines. The flame shape obtained theoretically is also shown by the solid line.

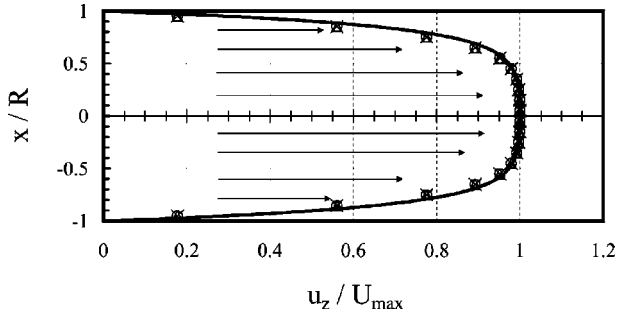

FIG. 7. The velocity profile u_z scaled by the amplitude $U_{\max}$. The solid line shows the theoretical result (8). The markers correspond to the simulation results for Re=50, Pr=1 at the distances $10R,20R,35R$ (circles, triangles and crosses) from the flame at the time instance $tU_f/R=1.15$. The arrows illustrate the direction of the flow.

theory and the simulations in Fig. 6. First, in the simulations the flame front becomes wider close to the walls in comparison with the central part of the tube. Such an effect is, obviously, beyond the scope of the model of an infinitely thin front used in the theory. Second, we can observe a little trough close to the tube axis in the simulations, while the theory predicts a flat top of the flame front. A similar trough was observed in earlier simulations of the accelerating flames [30,31]. At present we cannot say for sure what the origin of the trough is. One possibility is that it develops because of the particular initial conditions, which were basically the same in the present paper and in the earlier papers [30,31]. The other possibility is that the trough is a footprint of the DL instability developing at the locally planar part of the flame front close to the tube axis. We would like to stress that the locally planar part of the flame is accelerating. In the accelerating reference frame the flame experiences an effective gravity pointing from the heavy fuel mixture to the light burning products. As a result the DL instability at the planar flame top must be enhanced by the Rayleigh-Taylor instability similar to the studies [23–25]. The flow configuration in that case resembles also the hydrodynamic instability (DL plus Rayleigh-Taylor) in the ablation flow of the inertial confined fusion [39].

Figure 6 presents also the streamlines of the flow produced by the accelerating flame. As we can see, the streamlines are parallel to the tube walls with a good accuracy everywhere up to the flame front, which justifies the assumption of the plane-parallel flow made in the theory. To check this property of the flow quantitatively, in Fig. 7 we have presented the velocity distribution ahead of the flame front for the simulation run with Re=25, Pr=1 at the time instance $tU_f/R=1.15$. The markers correspond to the simulation results at the distances $10R;20R;35R$ (circles, triangles, and crosses) from the flame. The arrows illustrate the direction of the flow. As we can see, the velocity profile does not change as we move away from the flame front. This is true, of course, as long as the distance is not too large, for which even tiny effects of gas compression and nonzero Mach number may become noticeable. Figure 7 compares also the numerical results and the theoretical predictions for the velocity profile (8). We can see that the theory agrees quite well with the numerical simulations.

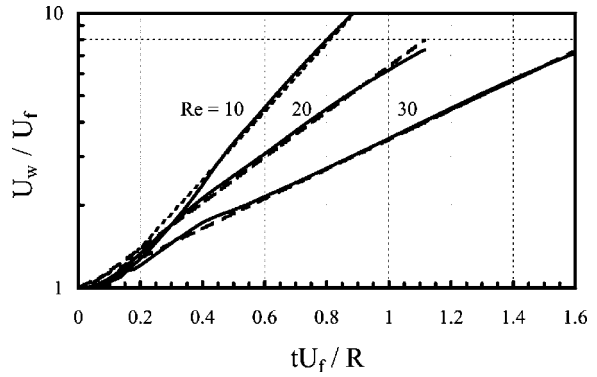

FIG. 8. The burning rate U_w/U_f versus time for Re=10,20 (Pr=1) and Re=30 (Pr=0.5). The solid lines show the simulation results, the dashed lines show the respective exponential approximations used to calculate the acceleration rate.

Modifications of the flame shape shown in Fig. 5 produce some increase in the burning rate U_w. Time variations of the scaled burning rate U_w/U_f are presented in Fig. 8 by solid lines for different simulation parameters Re=10,20 (Pr=1) and Re=30 (Pr=0.5). As we can see, in the initial stage of small flame curvature $U_w/U_f-1 \ll 1$ a flame accelerates in a relatively slow regime. However, quite soon the acceleration becomes exponential. Roughly speaking, we may treat the acceleration regime as exponential when $[1+(\partial f/\partial \eta)^2]^{1/2} \approx |\partial f/\partial \eta|$, which holds with the accuracy of 25% already for $|\partial f/\partial \eta| \approx 2$. Indeed, as we can see in Fig. 8, the acceleration regime becomes exponential with rather good accuracy for $U_w/U_f=2-2.5$. The dashed lines in Fig. 8 show the respective exponential approximations for every plot. Because of the exponential acceleration the burning rate U_w/U_f increased by order of magnitude in a rather short time determined by the inverse acceleration rate. The increase of the burning rate could be even stronger, but in that case we would be out of the laminar regime. We would like to stress that the velocity increase obtained in the flame acceleration is much stronger than that provided by the DL instability. For comparison, in the same geometry but with ideal slip at the walls the DL instability increases the burning rate only by (20–30)% relative to U_f [23,25,38]. Figure 9 shows the acceleration rate σ versus the Reynolds number, the solid line

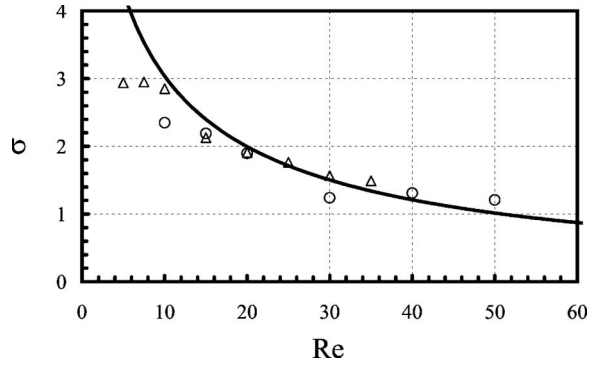

FIG. 9. The acceleration rate σ versus the Reynolds number Re. The solid line shows the theoretical result (21), the markers present the simulation results for Pr=0.5 (circles) and Pr=1 (triangles).

and the markers present the theory, Eq. (21), and the simulation results. As we can see, the theory predicts the acceleration rate quite well both qualitatively and quantitatively. In agreement with the theory we observe strong decrease of the acceleration rate with the Reynolds number. The numerical results deviate from the theoretical predictions only for narrow tubes $R/L_f \leqslant 7$, when the finite flame thickness influences the acceleration.

V. SUMMARY AND DISCUSSION

In the present paper we have developed the analytical theory of flame acceleration in tubes. In agreement with Shelkin's idea, the flame accelerates because of the nonslip boundary conditions at the tube walls. The developed theory predicts the main features of flame acceleration: the exponential in time regime of acceleration (6); the acceleration rate (21); the flame shape (17); and the velocity profile in the flow pushed by the flame front (8). According to the theory, the acceleration rate decreases with the Reynolds number of the flow (for example, with increase of the tube width).

We have validated the analytical theory by extensive direct numerical simulations of the combustion equations including transport processes and chemical kinetics. Predictions of the analytical theory are in a good agreement with the numerical results.

It is also interesting to compare flame acceleration because of the nonslip at the tube walls to other "candidates" for the explanation of accelerating flames (we use the same dimensionless units as in Sec. II). One of the candidates was the DL instability. According to the linear theory of the DL instability, small perturbations of an infinitely thin flame front grow as $f \propto \exp(\sigma\tau)$ with the instability growth rate [1,4,25]

$$\sigma = \frac{\pi\Theta}{\Theta+1}[(\Theta+1-1/\Theta)^{1/2}-1]. \tag{39}$$

For example, taking $\Theta=8$ we obtain $\sigma=5.5$, which is larger than the acceleration rate obtained in the present paper. However, a planar-in-average flame front accelerates because of the DL instability only during a very short time. As the flame velocity increases, the Huygens nonlinear mechanism reduces strongly the acceleration rate and eventually stops the acceleration. The acceleration goes on until the velocity of flame propagation becomes about $U_w/U_f=1.2-1.3$ for the tube width considered in the present paper. On the contrary, flame acceleration because of the nonslip at the walls is not limited in time, which makes it much more interesting from the point of view of the detonation triggering. The DL instability can ignite detonation only in the case of artificially large initial values of the Mach number.

The other interesting mechanism of flame acceleration was considered in Ref. [28] in the context of the tulip flame phenomenon. This mechanism concerns the initial stage of flame propagation in a tube, when a spherically in-average flame front just after ignition develops into a front, which is planar-in-average. At that stage the flame has not touched the walls yet, and the flame shape resembles a finger. As it was shown in Ref. [28], in that case the distance from the finger

bottom to the tip grows exponentially in time with the acceleration rate $\sigma=2\Theta$, which leads to strong acceleration of the flame front in the case of realistic thermal expansion (e.g., $\sigma=16$ for $\Theta=8$). However, the described mechanism works only during a very short time. According to Ref. [28], the flame front changes from spherical to "finger"-shaped at the time instant about $\tau_{\mathrm{sph}}\approx 0.1$, and the flame touches the wall at $\tau_{\mathrm{wall}}\approx 0.26$. The whole time of flame acceleration is limited from above by $\tau_{\mathrm{wall}}-\tau_{\mathrm{sph}}\approx 0.16$. Therefore, unlike the DL instability, such a mechanism can provide increase of the burning rate U_w/U_f by order of magnitude. For sufficiently fast flames such as burning in hydrogen-oxygen mixtures, it can be responsible for the detonation triggering. Still, in the case of usual slow flames it cannot provide long-time working acceleration like the acceleration because of the nonslip at the walls.

Finally, we point out how our theory explains accelerating turbulent flames observed experimentally [1,3–8]. First, our theory predicts strong decrease of the acceleration rate σ with the Reynolds number, which agrees with experiments and explains why the acceleration is very slow in tubes with smooth walls. However, it was noticed already by Shelkin [3] that rough walls make the acceleration much faster. Indeed, in that case the average profile of the turbulent velocity does not depend on the Reynolds number and may be approximated by the logarithmic function [2] $\ln(y/d)$, where y is the distance from the wall and d is the characteristic size of the wall nonuniformities. Replacing the laminar velocity profile by the logarithmic function, and the laminar flame velocity U_f by the average turbulent flame speed U_t we evaluate the dimensionless acceleration rate σ from Eq. (21) rewritten for the cylindrical geometry. Unfortunately, we are not aware of any experimental measurements of σ; the experimental results concern typically the dimensional characteristic length or time of flame acceleration [1,3–8]. These values, of course, depend on σ, but they also involve the turbulent flame speed U_t, which by itself is an important problem of hydrodynamics and combustion science waiting for solution. Particularly, U_t depends on turbulent intensity, which increases during the flame acceleration because of the increase of the Reynolds number. We hope that theoretical understanding of the flame acceleration achieved in the present paper will provide a good platform for more elaborated experiments.

It is not clear if the flame acceleration investigated in the present paper is possible in real tubes in the laminar regime of burning. Formally, the tube widths studied here are pretty narrow, about several millimeters. Tubes of this type are used in combustion experiments quite seldom, mostly in the context of flammability limits [1]. Obviously, in such a narrow tube one cannot neglect heat loss to the walls as we did in the present analysis. As pointed out by the referee, the acceleration rate predicted in the present paper is of the same order of magnitude as the cooling rate to the walls. Therefore, trying to observe acceleration of laminar flames in narrow tubes, one may obtain the acceleration rate much smaller than the values predicted in the present paper, if there will be any acceleration at all. As an alternative, one may observe flame oscillations in a tube with strong cooling at the walls similar to Ref. [31].

ACKNOWLEDGMENTS

The work was supported by the Swedish Research Foundation and by the Kempe Foundation. We thank Gregory Sivashinsky, Lennart Stenflo, Alexander Talyzin, and Gert Brodin for useful discussions.

[1] F. A. Williams, *Combustion Theory* (Benjamin, Redwood City, CA, 1985).
[2] L. D. Landau and E. M. Lifshitz, *Fluid Mechanics* (Pergamon Press, Oxford, 1989).
[3] K. I. Shelkin, Zh. Eksp. Teor. Fiz. **10**, 823 (1940).
[4] Ya. B. Zeldovich, G. I. Barenblatt, V. B. Librovich, and G. M. Makhviladze, *Mathematical Theory of Combustion and Explosion* (Consultants Bureau, New York, 1985).
[5] J. E. Shepherd and J. H. S. Lee, in *Major Research Topics in Combustion* (Springer Verlag, Hampton, VA, 1992), Vol. 439.
[6] S. Kerampran, D. Desbordes, and B. Veyssiere, Combust. Sci. Technol. **158**, 71 (2000).
[7] G. Roy, S. Frolov, A. Borisov, and D. Netzer, Prog. Energy Combust. Sci. **30**, 545 (2004).
[8] V. E. Tangirala, A. J. Dean, D. M. Chapin, P. F. Pinard, and B. Varatharajan, Combust. Sci. Technol. **176**, 1779 (2004).
[9] P. Clavin and F. A. Williams, J. Fluid Mech. **90**, 589 (1979).
[10] V. Yakhot, Combust. Sci. Technol. **60**, 191 (1988).
[11] A. R. Kerstein, W. T. Ashurst, and F. A. Williams, Phys. Rev. A **37**, R2728 (1988).
[12] R. G. Abdel-Gayed, D. Bradley, and M. Lawes, Proc. R. Soc. London, Ser. A **414**, 389 (1987).
[13] R. C. Aldredge and F. A. Williams, J. Fluid Mech. **228**, 487 (1991).
[14] A. Pocheau, Phys. Rev. E **49**, 1109 (1994).
[15] R. C. Aldredge, V. Vaezi, and P. D. Ronney, Combust. Flame **115**, 395 (1998).
[16] H. Kobayashi and H. Kawazoe, The 28th Symposium (International) on Combustion (The Combustion Institute, 2000), p. 375.
[17] B. Denet, Combust. Theory Modell. **5**, 85 (2001).
[18] D. Veynante and L. Vervisch, Prog. Energy Combust. Sci. **28**, 193 (2002).
[19] T. Lee and S. Lee, Combust. Flame **132**, 492 (2003).
[20] V. Bychkov, Phys. Rev. E **68**, 066304 (2003).
[21] H. Chen, S. Kandasamy, S. Orszag, R. Shock, S. Succi, and V. Yakhot, Science **301**, 633 (2003).
[22] B. Hof, C. van Doorne, J. Westerweel, F. Nieuwstadt, H. Faisst, B. Eckhardt, H. Wedin, R. Kerswell, and F. Waleffe, Science **305**, 1594 (2004).
[23] V. V Bychkov, S. M. Golberg, M. A. Liberman, and L. E. Eriksson, Phys. Rev. E **54**, 3713 (1996).
[24] V. Bychkov, S. Golberg, M. Liberman, A. Kleev, and L. E. Eriksson, Combust. Sci. Technol. **129**, 217 (1997).

[25] V. Bychkov and M. Liberman, Phys. Rep. **325**, 115 (2000).
[26] Y. Gostintsev, A. Istratov, and Y. Shulenin, Combust., Explos. Shock Waves **24**, 563 (1988).
[27] D. Bradley, T. M. Cresswell, and J. S. Puttock, Combust. Flame **124**, 5551 (2001).
[28] C. Clanet and G. Searby, Combust. Flame **105**, 225 (1996).
[29] I. Brailovsky and G. Sivashinsky, Combust. Flame **122**, 492 (2000).
[30] L. Kagan and G. Sivashinsky, Combust. Flame **134**, 389 (2003).
[31] J. D. Ott, E. S. Oran, and J. D. Anderson, AIAA J. **41**, 1391 (2003).
[32] Ya. B. Zeldovich, A. G. Istratov, N. I. Kidin, and V. B. Librovich, Combust. Sci. Technol. **24**, 1 (1980).
[33] V. Bychkov, Phys. Fluids **10**, 2091 (1998).
[34] P. Pelce, J. Phys. (France) **46**, 503 (1985).
[35] Z. Olami, B. Galanti, O. Kupervasser, and I. Procaccia, Phys. Rev. E **55**, 2649 (1997).
[36] B. Denet, Phys. Rev. E **59**, 2966 (1999).
[37] L. Kagan and G. Sivashinsky, Combust. Flame **120**, 222 (2000).
[38] O. V. Travnikov, V. V. Bychkov, and M. A. Liberman, Phys. Rev. E **61**, 468 (2000).
[39] V. Bychkov, S. Golberg, and M. Liberman, Phys. Plasmas **1**, 2976 (1994).